

Understanding the stagnation and burn of implosions on NIF

This content has been downloaded from IOPscience. Please scroll down to see the full text.

2016 J. Phys.: Conf. Ser. 688 012048

(<http://iopscience.iop.org/1742-6596/688/1/012048>)

View [the table of contents for this issue](#), or go to the [journal homepage](#) for more

Download details:

IP Address: 64.134.238.2

This content was downloaded on 06/04/2016 at 03:27

Please note that [terms and conditions apply](#).

Understanding the stagnation and burn of implosions on NIF

J D Kilkenny⁵, J A Caggiano¹, R Hatarik¹, J P Knauer², D B Sayre¹, B K Spears¹, S V Weber¹, C B Yeamans¹, C J Cerjan¹, L Divol¹, M J Eckart¹, V Yu Glebov², H W Herrmann³, S Le Pape¹, D H Munro¹, G P Grim³, O S Jones¹, L Berzak-Hopkins¹, M Gatu-Johnson⁴, A J Mackinnon¹, N B Meezan¹, D T Casey¹, J A Frenje⁴, J M Mcnaney¹, R Petrasso⁴, H Rinderknecht⁴, W Stoeffl¹ and A B Zylstra⁴.

¹Lawrence Livermore National Laboratory, Livermore, CA 94550, USA

²Laboratory for Laser Energetics, Univ. of Rochester, Rochester, NY 14623, USA

³Los Alamos National Laboratory, Los Alamos, NM 87545, USA

⁴Plasma Science and Fusion Center, Massachusetts Institute of Technology, Cambridge, MA 02139, USA

⁵General Atomics, San Diego, CA, 29186, USA

E-mail: kilkenny@fusion.gat.com

Abstract. : An improved set of nuclear diagnostics on NIF measures the properties of the stagnation plasma of implosions, including the drift velocity, areal density (ρr) anisotropy and carbon ρr of the compressed core. Two types of deuterium-tritium (DT) gas filled targets are imploded by shaped x-ray pulses, producing stagnated and burning DT cores of radial convergence (C_r) ~ 5 or ~ 20 . Comparison with two-dimensional modeling with inner and outer surface mix shows good agreement with nuclear measurements.

1. Introduction

The x-ray drive, inertial confinement fusion approach at the National Ignition Facility (NIF) uses x-rays to implode a multi-layered, spherical shell at the center of the hohlraum. For the ignition goal the radiation drive is shaped to launch 4 staged shocks to control the adiabat and to achieve high compression of the cryogenically layered fuel [1]. However for low foot ignition designs the measured capsule neutron yield is substantially lower than simulations [2]. It has been known for decades, based on theory [3] and experiments with high power lasers [4, 5] that implosions are unstable to the Rayleigh-Taylor (RT) instability which can lead to ablator material mixing into the hot spot and reducing the yield. In an effort to understand the yield discrepancy DT gas filled plastic capsules are imploded as simulants of the cryogenically layered implosions that are fielded in an “ignition” hohlraum [1]. The gas fill results in a lower convergence, less stressing implosion than a layered implosion. Improved nuclear diagnostics measure the drift velocities and carbon (from plastic ablaters) areal densities of the imploded cores as well as the normal attributes, yield, ion temperature, and down scattered fraction. With improved modelling good agreement with simulations is seen, for example the neutron yield agrees with simulations to $\sim 80\%$.

2. Gas Filled Implosions to Emulate Layered Implosions

Two types of gas filled implosions are discussed here. The first type is a set of x-ray drive “exploding pushers”. These easier implosions achieve low areal density with a high yield and a low drift velocity.



Described elsewhere [6] these are single shock, $C_r \sim 5$ x-ray driven implosion producing a well-understood stagnation plasma. Here they are used to test the upgraded diagnostics of section 3.

The second type is a set of higher convergence, $C_r \sim 20$, and more unstable implosions. The design consists of four shocks and a target like the layered implosions [1], but with a thicker plastic shell to emulate the DT ice, and a DT gas fill. Simulations of this second type represent the conditions of the actual experiment, including the as-shot capsule metrology, capsule surface roughness, and the tent (the thin foils which hold the capsule in the hohlraum) as seeds for the growth of hydrodynamic instabilities. The 2D zoning resolves up to a spherical harmonic mode of $l=100$. As in reference [2] the drive is reduced to match the measured implosion timing, kinematics, and low-mode asymmetry.

3. The improved set of neutron diagnostics

Recent upgrades to NIF's nuclear diagnostics allow better measurements of the properties of implosions. The upgrades were validated on the $C_r \sim 5$ single-shock implosions, and then used on the $C_r \sim 20$ four-shock implosions.

3.1. Neutron Time of Flight (nToF) detectors: The initial set of NIF diagnostic had two spectrally resolving nToFs [8] with 20 m neutron flight paths. A recently added nToF with an 18 m flight path and near the south pole of the chamber gives three nearly orthogonal views of the implosion with spectrally resolving detectors. Modifications to the original design on all three include faster scintillators [9] and faster recording, allowing measurements of the drift velocity of the neutron source and the carbon back-scattering edges [10]. As before these nToFs also measure yield, "ion temperature T_{ion} " and down scattered neutrons as described in reference [11]. Note that the temporal and spatial averaging of the nToFs gives a perceived "ion temperature" which includes an inhomogeneous velocity contribution as well as the thermal motion. However " T_{ion} " from the simulations in this paper also includes this factor—at least to the fidelity of the simulation.

Additionally these nToFs measure the average drift velocity for the first time. For example if the neutron emitting imploded core has an average drift velocity towards a detector it will slightly increase the neutron velocity in the laboratory frame resulting in an earlier arrival. To demonstrate this ability to measure drift velocities three shots were performed with a symmetric drive, a 4% upwards, and 4% downwards drive asymmetry as shown in figure 1.

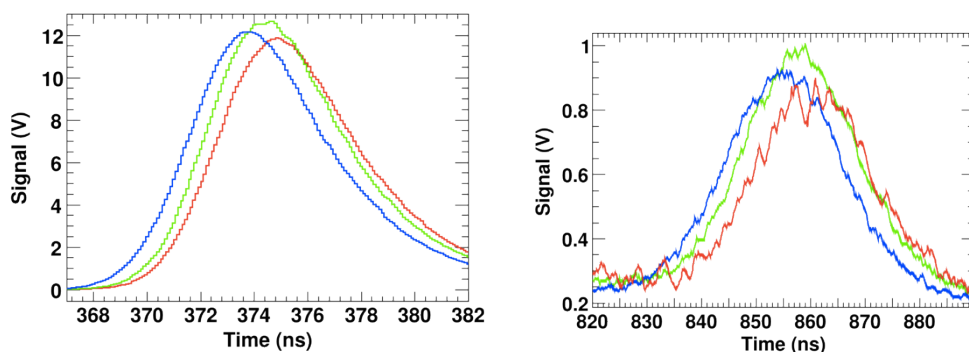


Figure 1: nToF signals near the south pole for DT neutrons (left) and DD neutrons (right). The blue trace is for a deliberate downwards P_1 drive asymmetry of 4% (N130625), the green trace is for a symmetric drive (N130507) and the red trace is for a deliberate upwards P_1 drive asymmetry of 4% (N130814).

To calculate the drift velocities the bang time, when neutron production peaks is measured by time resolved x-ray emission and DT-fusion gamma-ray emission to an accuracy of about 100 psec. The velocity of the neutrons in the lab frame uses the measured T_{ion} [12]. The drift velocities are obtained by fitting the arrival time for both the DT and the DD neutrons and in km/s are 76, 1, and -76 and

62, -12 and -78 respectively for the down, symmetric and up implosions. The drift velocities increase, are close to zero, and decrease as expected with the imposed asymmetry. Additionally the DD and DT velocities are close to agreeing within the fitting error of ~ 10 km/s.

3.2. Flange Neutron Activation Diagnostic System (fNADS): The fNADS system on NIF [13] uses $^{90}\text{Zr}(n,2n)^{89}\text{Zr}$ activation measured by zirconium (Zr) slugs mounted on 19 target chamber flange covers. Measured activation anisotropy can be due to anisotropy in the flux of un-scattered neutrons or a drift velocity as this activation cross-section increases with neutron energy. The relative variation in the activation, A/A_{ave} for the two asymmetric experiments of section 3.1 are shown in Figure 2 showing an increase in activation in the direction of motion. If the measured velocities are used to correct the anisotropy in yield the remaining anisotropy due to areal density variations is obtained. Some level of consistency with the down-scattered ratio is obtained but is under further investigation.

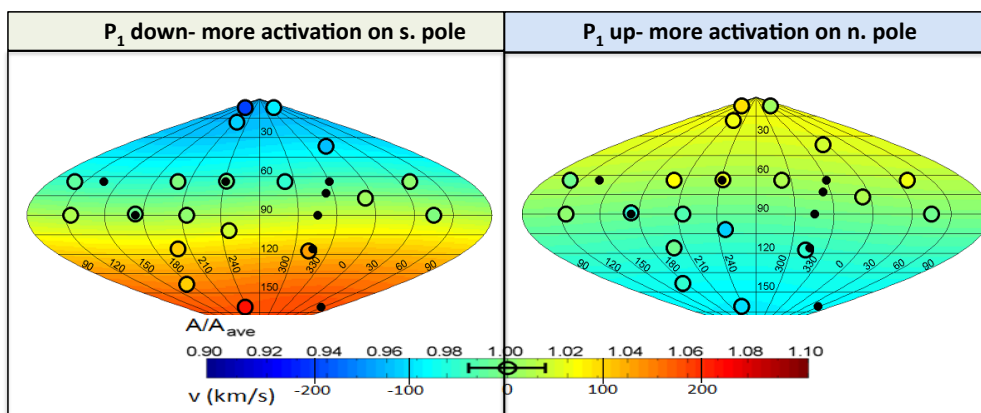


Figure 2: The variation in relative activation A/A_{ave} for the asymmetric experiments of section 3.1.

3.3. The Gamma Reaction History (GRH) detector: In addition to the DT-fusion gamma rays the GRH diagnostic measures the 4.4 MeV gamma line from the $^{12}\text{C}(n,n'\gamma)$ reaction [14]. The GRH was absolutely calibrated by measuring the 4.4 MeV γ s emitted from a puck of carbon held 5.5 cm from a calibrated exploding pusher target. On the implosions described here, carbon nuclei remaining from the plastic ablator are excited by 14 MeV DT neutrons and emit 4.4 MeV γ s, thus measuring the ^{12}C areal density. Figure 3 shows the good agreement between GRH measured and calculated (Hydra) 4.4 MeV γ yields for the single shock (bottom left) and four shock implosions (top right).

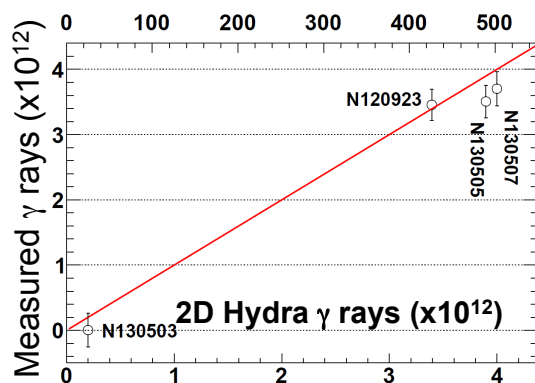


Figure 3: Measured and calculated carbon γ yields from GRH. Upper horizontal axis is the ^{12}C pr (mg/cm 2).

4. Comparison of experiments with simulations and conclusions

The DD and DT yields are compared to simulations in figure 4. These simulations follow those in reference [2] but with a mix prescription for the inner surface as it is decelerated by the gas, representing 0.05 times the distance to the fall line. The fall line fraction is a simple parameterized prescription to introduce time dependent mix based on the Read and Youngs [7] mix measurements. The yields are calculated in 1D, 2D and in 2D with this mix prescription showing excellent agreement for the single shock implosions and good agreement (80%) for the four-shock system. The nToF-derived T_{ion} from the DD and DT burn is also compared to simulations post processed for a simulated T_{ion} in figure 4 showing excellent agreement with the simulations. The stronger dependence on T_{ion} for the DT reaction over time and spatial averaging of the nToFs gives a larger measured " T_{ion} " from the DT reaction than the DD reaction. The differences are 400 eV and 200 eV for the single and four shock implosions respectively.

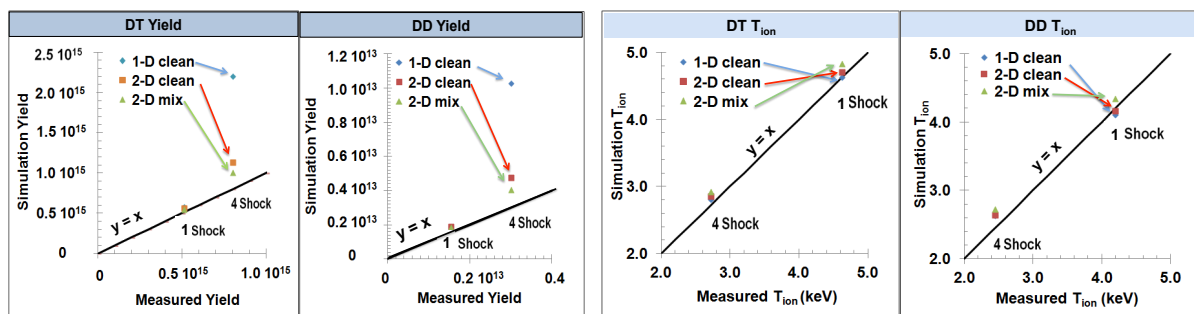


Figure 4: Calculated and measured DT and DD neutron yields (left) and corresponding instrumentally measured T_{ions} for the one shock implosion (N130503) and a four shock implosion (N130505).

This work was performed under the auspices of the U.S. Department of Energy by Lawrence Livermore National Laboratory under Contract DE-AC52-07NA27344.

References

- [1] M. J. Edwards et. al., Phys. of Plasmas **20**, 070501 (2012).
- [2] D. S. Clark et. al., Phys. of Plasmas **20**, 056318 (2013).
- [3] J.D. Lindl and W.C. Mead, Phys. Rev. Lett. **34**, 1273 (1975).
- [4] J.S. Wark, J.D. Kilkenny, et. al., Appl. Phys. Lett. **48**, 969 (1987).
- [5] J. D. Kilkenny, Phys. Fluids **B2**, 1400 (1990).
- [6] S. LePape, submitted to Phys. Rev. Lett.
- [7] K. I. Read, 1984 *Physica D* **12**, 45 and D. L. Youngs, 1984 *Physica D* **12**, 32.
- [8] V. Yu. Glebov et. al., Rev. Sci. Instrumen. **81**, 10D325 (2010).
- [9] R. Hatarik et. al., Rev. Sci. Instrumen. **83**, 10D911 (2012).
- [10] C. J. Forrest et. al., Rev. Sci. Instrumen. **83**, 10D919 (2012).
- [11] R. A. Lerche et. al., Rev. Sci. Instrumen. **81**, 10D319 (2010).
- [12] L. Ballabio, J. Kallne and G. Gorini, Nuclear Fusion, **38**, 1723 (1999).
- [13] C. B. Yeamans et. al., Rev. Sci. Instrumen. **83**, 10D313 (2012).
- [14] D. B. Sayre et. al., Rev. Sci. Instrumen. **83**, 10D905 (2012).